

# Accurate calculation of the transverse anisotropy of a magnetic domain wall in perpendicularly magnetized multilayers

Felix Büttner,<sup>1,2,3,\*</sup> Benjamin Krüger,<sup>1,\*</sup> Stefan Eisebitt,<sup>3,4</sup> and Mathias Kläui<sup>1,2</sup>

<sup>1</sup>*Institute of Physics, Johannes-Gutenberg-Universität Mainz, Staudinger Weg 7, 55128 Mainz, Germany*

<sup>2</sup>*Graduate School Materials Science in Mainz, Staudinger Weg 9, 55128 Mainz, Germany*

<sup>3</sup>*Institut für Optik und Atomare Physik, Technische Universität Berlin, Straße des 17. Juni 135, 10623 Berlin, Germany*

<sup>4</sup>*Helmholtz-Zentrum Berlin für Materialien und Energie GmbH, Hahn-Meitner-Platz 1, 14109 Berlin, Germany*

(Received 2 March 2015; revised manuscript received 25 May 2015; published 5 August 2015; corrected 13 August 2015)

Bloch domain walls are the most common type of transition between two out-of-plane magnetized domains (one magnetized upwards, one downwards) in films with perpendicular magnetic anisotropy. The rotation of the spins of such domain walls in the plane of the film requires energy, which is described by an effective anisotropy, the so-called transverse or hard axis anisotropy  $K_{\perp}$ . This anisotropy and the related Döring mass density of the domain wall are key parameters of the one-dimensional model to describe the motion of magnetic domain walls. In particular, the critical field strength or current density where oscillatory domain wall motion sets in (Walker breakdown) is directly proportional to  $K_{\perp}$ . So far, no general framework is available to determine  $K_{\perp}$  from static characterizations such as magnetometry measurements. Here, we derive a universal analytical expression to calculate the transverse anisotropy constant for the important class of perpendicular magnetic multilayers. All the required input parameters of the model, such as the number of repeats, the thickness of a single magnetic layer, and the layer periodicity, as well as the effective perpendicular anisotropy, the saturation magnetization, and the static domain wall width are accessible by static sample characterizations. We apply our model to a widely used multilayer system and find that the effective transverse anisotropy constant is a factor of seven different from that when using the conventional approximations, showing the importance of using our analysis scheme. Our model is also applicable to domain walls in materials with Dzyaloshinskii-Moriya interaction (DMI). The accurate knowledge of  $K_{\perp}$  is needed to determine other unknown parameters from measurements, such as the DMI strength or the spin polarization of the spin current in current-induced domain wall motion experiments.

DOI: [10.1103/PhysRevB.92.054408](https://doi.org/10.1103/PhysRevB.92.054408)

PACS number(s): 75.78.Fg, 75.70.-i

## I. INTRODUCTION

Multilayers with perpendicular magnetic anisotropy (PMA) are widely used in research as well as in applications [1–7]. A particular focus of the research today is the investigation of domain wall dynamics in such materials. Theoretically, the dynamics of domain walls is often described by the one-dimensional model [8–10]. In this model, the tilt angle  $\psi$  of the spins in the domain wall with respect to the domain wall plane is used as the conjugated momentum to the domain wall position  $q$ . The energy associated with a change of  $\psi$  can be described by an effective uniaxial anisotropy, the so-called transverse anisotropy (also called hard axis anisotropy [6,9] or domain wall demagnetizing energy [10]) with the anisotropy constant  $K_{\perp}$  [2–11]. In general, this anisotropy acts as an energy reservoir that leads to domain wall quasiparticle behavior, such as domain wall inertia [12] due to an effective domain wall mass [13].

The transverse anisotropy constant is a key parameter to describe domain wall dynamics: it is proportional to the critical excitation strength (field or current) beyond which the domain wall becomes nonsteady (Walker breakdown) [2,9,10,14] and it is related to the inertia of the domain wall through the Döring

mass density  $m_D$  through the simple relation [8,15]

$$m_D = \frac{M_s^2(1 + \alpha^2)}{K_{\perp}\gamma^2\Delta_0}, \quad (1)$$

where  $\alpha$  is the Gilbert damping,  $\gamma = 1.76 \times 10^{11}$  As/kg is the gyromagnetic ratio,  $\Delta_0 = \sqrt{A/K_{u,\text{eff}}}$  the static domain wall width,  $A$  is the exchange stiffness, and  $K_{u,\text{eff}}$  the effective perpendicular anisotropy constant. Note that  $K_{u,\text{eff}}$  is different from the crystal anisotropy  $K_u$  due to the out-of-plane stray field energy [1,16,17]. A discussion on how to extract  $K_{u,\text{eff}}$  and  $K_u$  from hysteresis loop data can be found in Ref. [1].

In the literature, the transverse anisotropy is often expressed as an effective magnetic field  $H_K$  or via the demagnetization tensor  $N$ . The conversion in SI units reads

$$H_K = \frac{2K_{\perp}}{\mu_0 M_s}, \quad (2)$$

$$N_x = \frac{2K_{\perp}}{\mu_0 M_s^2}, \quad (3)$$

where we have assumed a thin film geometry with vanishing in-plane demagnetization energy for a Bloch domain wall ( $N_y = 0$ ) [10].  $\mu_0$  is the vacuum permeability.

The effective transverse anisotropy constant  $K_{\perp}$  is not directly accessible from static sample characterization. Existing theories predict  $K_{\perp}$  only for homogeneous magnetic materials and only in the limits of infinitely thick samples (bulk samples) [8], where  $K_{\perp} = 1/2\mu_0 M_s^2$ , and for ultra-thin films of thickness  $\mathcal{T} \rightarrow 0$  [18], where  $K_{\perp} = \ln(2)\mathcal{T}\mu_0 M_s^2/(2\pi\Delta_0)$ .

\*These authors contributed equally to this work.

†felixbuettner@gmail.com

‡bkrueger@uni-mainz.de

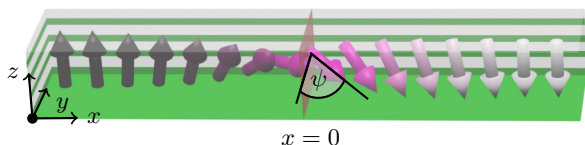


FIG. 1. (Color online) Magnetization profile in a multilayer material, as assumed by the calculations in this paper. Magnetic layers are depicted in green and nonmagnetic layers in gray. The shown material has  $\mathcal{N} = 4$ . The profile shows a domain wall at  $x = 0$ , separating a domain where all magnetic moments point upwards (black arrows at the left side of the picture) from a domain where all magnetic moments point downwards (white arrows at the right side of the picture). The angle in the  $x$ - $y$  plane is the so-called transverse angle  $\psi$ . This angle is uniform for all magnetic moments.

As shown in this paper, these approximations yield significantly inaccurate results if applied to typical multilayer films, which are the application-relevant systems.

In this paper, we present rigorous calculations of the magnetostatic energy of a multilayer system with a domain wall, from which we obtain analytical expressions for the transverse anisotropy constant  $K_{\perp}$  as a function of the thickness of a single magnetic layer  $\mathcal{T}$  (thickness of one green layer in Fig. 1), the multilayer periodicity  $\mathcal{P}$  (combined thickness of one green and one gray layer in Fig. 1), the number of repeats  $\mathcal{N}$  ( $\mathcal{N} = 4$  in Fig. 1), the static domain wall width  $\Delta_0$ , and the saturation magnetization  $M_s$ . Note that the effective perpendicular anisotropy enters only indirectly through  $\Delta_0$ . We find that the saturation magnetization enters the equation only as a simple linear scaling factor and that  $\Delta_0$ ,  $\mathcal{P}$ , and  $\mathcal{T}$  enter only in the ratios  $p := \mathcal{P}/(2\pi\Delta_0)$ ,  $t := \mathcal{T}/(2\pi\Delta_0)$ , and  $\tau := \mathcal{P}/\mathcal{T}$ . We provide accurate equations for  $K_{\perp}$  as the main result of this paper in Eq. (42) and we will show that

$$K_{\perp}(t, p, \mathcal{N}) \approx \mu_0 M_s^2 \frac{d^2 f(\tau, \mathcal{N}) + d \ln(2)}{2d^2 f(\tau, \mathcal{N}) + d g(\tau, \mathcal{N}) + 1} \quad (4)$$

with

$$\begin{aligned} f(\tau, \mathcal{N}) &= (0.9\tau - 0.76)/\mathcal{N} \\ g(\tau, \mathcal{N}) &= \tau[1.8 - 0.05 \ln(\mathcal{N} + 12) + 0.05 \ln(\tau)] \\ d &= t\mathcal{N} \end{aligned} \quad (5)$$

approximates the exact result with less than 9% error for  $10^{-4} \leq t\mathcal{N} \leq 10^5$ ,  $1 < \mathcal{N} \leq 128$ , and  $1.25 \leq \tau \leq 8$  and for  $\tau = 1$  and  $\mathcal{N} = 1$ , which covers many systems that are intensely investigated today.

## II. GENERAL EQUATIONS

The transverse anisotropy constant is a parameter of the one-dimensional (1D) model. The following calculations are based on this model, which assumes the presence of a single, straight domain wall in the  $y$ - $z$  plane with the magnetization profile

$$M_x(x) = M_s \cosh^{-1}(x/\Delta) \sin(\psi), \quad (6)$$

$$M_y(x) = M_s \cosh^{-1}(x/\Delta) \cos(\psi), \quad (7)$$

$$M_z(x) = M_s \tanh(x/\Delta), \quad (8)$$

as depicted in Fig. 1. This is the general profile that describes both the ground state as well as the shape during the motion of a domain wall in an infinite magnetic plane, assuming only that this domain wall separates one domain where the magnetization points upwards at  $x = -\infty$  from one where the magnetization points downwards at  $x = +\infty$  [8,16]. For structures of finite width, the spins at the boundary follow a different profile, which becomes significant if the width of the structure becomes smaller than approximately five times the full domain wall width  $2\pi\Delta_0$  [7].

In Eqs. (6)–(8),  $\mathbf{M} = (M_x, M_y, M_z)$  is the local magnetization,  $M_s = |\mathbf{M}|$  is the saturation magnetization,  $\Delta = \Delta(\psi)$  is the domain wall width parameter, and  $\psi$  is the transverse (domain wall) angle. The magnetization is homogeneous along the wall, i.e., it does not depend on  $y$  and  $z$ . The magnetostatic energy density  $\sigma_d$  of such a domain wall (energy per unit area of the wall) is symmetric in  $\psi$  and therefore can be described as a function of  $s := \sin^2 \psi$ . Also, the magnetostatic energy can be read as a uniaxial anisotropy with the hard axis along the  $x$  direction. The general formula for such a uniaxial anisotropy reads

$$\sigma_d(s) = C + K_{\perp} \int dx (M_x/M_s)^2 + \mathcal{O}(s^2) \quad (9)$$

$$= C + 2\Delta_0 K_{\perp} s + \mathcal{O}(s^2), \quad (10)$$

where  $C$  is a constant and  $K_{\perp}$  is the leading-order anisotropy constant. The first-order partial derivative of Eq. (10) at  $s = 0$  yields  $K_{\perp}$ :

$$K_{\perp} = \frac{\sigma_d^{(1)}}{2\Delta_0}, \quad (11)$$

where the superscript  $(1)$  denotes the partial derivative with respect to  $s$  at  $s = 0$ . We will hence derive a formula to calculate the magnetostatic energy  $\sigma_d^{(1)}$ .

## III. MAGNETOSTATIC ENERGY DENSITY

In the following, we calculate the magnetostatic energy density  $\sigma_d$  and, in particular, the first-order partial derivative  $\sigma_d^{(1)}$ . We consider a thin film multilayer system of length  $\mathcal{L}$  ( $x$  direction) and width  $\mathcal{W}$  ( $y$  direction) in the limit  $\mathcal{L}, \mathcal{W} \rightarrow \infty$ , which is a reasonably accurate approximation if  $\mathcal{L}, \mathcal{W} \gg \Delta_0$ . In micromagnetic simulations, this situation can be realized by employing periodic boundary conditions in the  $x$  and  $y$  direction. Temporarily, we will treat for the calculation the width as a finite value and set it to infinity at a later stage. The ground state of such a perpendicular magnetic film is characterized by  $s = 0$ . As in the 1D model, we will assume the presence of a single domain wall in the  $y$ - $z$  plane at  $x = 0$ . However, now we have the additional  $y$  dependency of the finite width and the  $z$  dependency of the multilayer, which we describe as follows:

$$M_x(x, y, z) = M_x(x)w(y) \sum_{j=0}^{\mathcal{N}-1} v(z - j\mathcal{P}), \quad (12)$$

$$M_y(x, y, z) = M_y(x)w(y) \sum_{j=0}^{\mathcal{N}-1} v(z - j\mathcal{P}), \quad (13)$$

$$M_z(x, y, z) = M_z(x)w(y) \sum_{j=0}^{\mathcal{N}-1} v(z - j\mathcal{P}), \quad (14)$$

$$w(y) = \theta(\mathcal{W}/2 - |y - \mathcal{W}/2|), \quad (15)$$

$$v(z) = \theta(\mathcal{T}/2 - |z - \mathcal{T}/2|). \quad (16)$$

Here,  $\theta$  is the heaviside function. The magnetostatic energy of a magnetization configuration  $\mathbf{M}(\mathbf{r})$  per unit domain wall area reads

$$\sigma_d(s) = \frac{\mu_0}{8\pi\mathcal{W}\mathcal{N}\mathcal{T}} \iint d^3\mathbf{r}d^3\mathbf{r}' \rho(\mathbf{r})\rho(\mathbf{r}') \frac{1}{|\mathbf{r} - \mathbf{r}'|}, \quad (17)$$

where  $\rho$  is the volume density of magnetic charges,  $\mathcal{W}$  is the width of the structure ( $y$  direction), and  $\mathcal{N}\mathcal{T}$  is the total thickness of the magnetic material ( $z$  direction). Magnetic charges arise from the divergence of the magnetization inside the volume (volume charges) and from the components of the magnetization perpendicular to the surfaces of the structure (surface charges). However, the surface charges do not explicitly depend on  $s$  and the interactions between volume charges and surface charges vanish when averaged over  $y$  and  $z$  for symmetry reasons since all charges are antisymmetric around  $\mathbf{r} = 0$ . Therefore, the only relevant charges are the volume charges

$$\rho(\mathbf{r}) = \sum_{j=0}^{\mathcal{N}-1} \rho_1(x, y, z - j\mathcal{P}), \quad (18)$$

$$\rho_1(\mathbf{r}) = \rho_1(x)w(y)v(z), \quad (19)$$

$$\rho_1(x) = -\text{div } \mathbf{M} = \frac{M_s}{\Delta} \sin(\psi) \frac{\tanh(x/\Delta)}{\cosh(x/\Delta)}. \quad (20)$$

To solve the stray field integral Eq. (17), we will first simplify the general form of the integral using the symmetry properties of the charge distribution Eq. (20) and use the explicit form of the charge distribution at a later stage. The kernel of the double sum in the integral

$$\begin{aligned} \sigma_d &= \frac{\mu_0}{8\pi\mathcal{W}\mathcal{N}\mathcal{T}} \iint d^3\mathbf{r}d^3\mathbf{r}' \\ &\times \sum_{i,j=0}^{\mathcal{N}-1} \rho_1(x, y, z - i\mathcal{P})\rho_1(x', y', z' - j\mathcal{P}) \frac{1}{|\mathbf{r} - \mathbf{r}'|} \end{aligned} \quad (21)$$

$$\begin{aligned} &= \frac{\mu_0}{8\pi\mathcal{W}\mathcal{N}\mathcal{T}} \iint d^3\mathbf{r}d^3\mathbf{r}' \rho_1(x, y, z)\rho_1(x', y', z') \\ &\times \sum_{i,j=0}^{\mathcal{N}-1} \frac{1}{|\mathbf{r} + i\mathcal{P}\mathbf{e}_z - \mathbf{r}' - j\mathcal{P}\mathbf{e}_z|} \end{aligned} \quad (22)$$

depends on  $i$  and  $j$  only in the form  $i - j$ . That is, we can reorder the double sum to just one over this difference  $(i - j) = (-\mathcal{N} + 1), \dots, \mathcal{N} - 1$  (which we will index again by  $j$ ) and a factor  $\mathcal{N} - |j|$  that counts how often the term  $j$  is represented in the original sum:

$$\begin{aligned} \sigma_d &= \frac{\mu_0}{8\pi\mathcal{W}\mathcal{N}\mathcal{T}} \iint d^3\mathbf{r}d^3\mathbf{r}' \rho_1(\mathbf{r})\rho_1(\mathbf{r}') \\ &\times \sum_{j=-\mathcal{N}+1}^{\mathcal{N}-1} \frac{\mathcal{N} - |j|}{|\mathbf{r} - \mathbf{r}' + j\mathcal{P}\mathbf{e}_z|}. \end{aligned} \quad (23)$$

The charge density  $\rho$  has only a trivial dependence on  $y$  and  $z$ . Hence, we can easily solve the integration with respect to  $y$  and  $y'$ , giving

$$\begin{aligned} \sigma_d &= \frac{\mu_0}{8\pi\mathcal{N}\mathcal{T}} \iint dx dx' \int_0^{\mathcal{T}} dz \int_0^{\mathcal{T}} dz' \rho_1(x)\rho_1(x') \\ &\times \sum_{j=-\mathcal{N}+1}^{\mathcal{N}-1} (\mathcal{N} - |j|) f_{\mathcal{W}}(x - x', z - z' + j\mathcal{P}) \end{aligned} \quad (24)$$

with

$$\begin{aligned} f_{\mathcal{W}}(x, z) &= \frac{1}{\mathcal{W}} \int_0^{\mathcal{W}} dy \int_0^{\mathcal{W}} dy' \left[ \frac{1}{\sqrt{(y - y')^2 + x^2 + z^2}} \right] \\ &= -2 + 2 \ln(2\mathcal{W}) - \ln(x^2 + z^2) + \mathcal{O}(\mathcal{W}^{-1}). \end{aligned} \quad (25)$$

The steps to solve the integral Eq. (25) are discussed in detail in Appendix A. The terms constant in  $x$  vanish with the integration over  $x$  because the magnetic charges are antisymmetric in  $x$ . That is, in the limit  $\mathcal{W} \rightarrow \infty$ ,

$$\begin{aligned} \sigma_d &= \frac{\mu_0}{8\pi\mathcal{N}\mathcal{T}} \sum_{j=-\mathcal{N}+1}^{\mathcal{N}-1} (\mathcal{N} - |j|) \int_0^{\mathcal{T}} dz \int_0^{\mathcal{T}} dz' \iint dx dx' \\ &\times \rho_1(x)\rho_1(x')h(x - x', z - z' + j\mathcal{P}) \end{aligned} \quad (27)$$

with

$$h(x, z) = -\ln(x^2 + z^2). \quad (28)$$

As outlined in Appendix B, the double integral over  $x$  and  $x'$  can be reduced to a single integral in Fourier space. The result reads (the hat denotes a Fourier transform with respect to the  $x$  coordinate):

$$\begin{aligned} \sigma_d^{(1)} &= \frac{\mu_0 M_s^2 \sqrt{2\pi}}{8\pi\mathcal{N}\mathcal{T}} \sum_{j=-\mathcal{N}+1}^{\mathcal{N}-1} (\mathcal{N} - |j|) \int_0^{\mathcal{T}} dz \int_0^{\mathcal{T}} dz' \\ &\times \int dk |\hat{\xi}(k)|^2 \hat{h}(k, z - z' + j\mathcal{P}), \end{aligned} \quad (29)$$

with

$$\xi(x) = \frac{1}{\Delta_0} \frac{\tanh(x/\Delta_0)}{\cosh(x/\Delta_0)}, \quad (30)$$

$$\hat{\xi}(k) = ik\Delta_0 \sqrt{\frac{\pi}{2}} \frac{1}{\cosh\left(\frac{\pi\Delta_0 k}{2}\right)}, \quad (31)$$

$$\hat{h}(k, z) = \sqrt{2\pi} \frac{1}{|k|} e^{-|zk|}. \quad (32)$$

The only term that depends on  $z$  is the function  $\hat{h}$ . The integration of this part with respect to  $z$  and  $z'$  is lengthy but not very involved, as shown in detail in Appendix C. The result reads

$$\begin{aligned} \sigma_d^{(1)} &= \frac{\mu_0 M_s^2 \Delta_0}{8t} \sum_{j=-\mathcal{N}+1}^{\mathcal{N}-1} \frac{\mathcal{N} - |j|}{\mathcal{N}} \sum_{i=-1}^1 (3|i| - 2) \\ &\times \int_0^{\infty} dq \frac{e^{-|jp+it|q} + |jp + it|q - 1}{q \cosh^2(q/4)}, \end{aligned} \quad (33)$$

where we have introduced the reduced variables  $q := 2\pi\Delta_0 k$ ,  $p := \frac{\mathcal{P}}{2\pi\Delta_0}$ , and  $t := \frac{\mathcal{T}}{2\pi\Delta_0}$ . The  $-1$  in the integral has

been added to make each integral finite; it cancels out in the sum over  $i$ . We have furthermore replaced the integral over all  $q$  by twice the integral over  $q$  from 0 to  $\infty$ . The integral

$$G(x) := \int_0^\infty dq \frac{e^{-xq} + xq - 1}{q \cosh^2(q/4)} \quad (34)$$

can be solved analytically, as shown in Appendix D. The final result reads

$$\sigma_d^{(1)} = \frac{\mu_0 M_s^2 \Delta_0}{8t} \sum_{j=-\mathcal{N}+1}^{\mathcal{N}-1} \frac{\mathcal{N} - |j|}{\mathcal{N}} \times (G(|jp + t|) + G(|jp - t|) - 2G(|jp|)), \quad (35)$$

where the function  $G(x)$  is explicitly given in Eq. (D10). This result is exact but very lengthy and difficult to evaluate. We will optimize the result for numerical evaluation in the next section.

#### IV. EVALUATION

For practical purposes, the evaluation of Eq. (35) is often computationally too expensive. Also, we note that Eq. (35) contains differences of  $G$ , which means that a numerical evaluation of  $G$  may yield dramatically wrong results just due to the finite precision of computer algebra and the error made cannot be estimated easily. We will therefore rewrite Eq. (35) to eliminate the differences to make it more robust for numerical evaluation. In the following steps, we use that  $jp \geq t$  for  $j > 0$  and that  $G(0) = 0$  to rewrite the sum over  $j$  and to eliminate the absolute signs in the arguments of  $G$ . Subsequently, we expand  $G(x)$  in a Taylor series around  $jp$ .

$$\sum_{j=-\mathcal{N}+1}^{\mathcal{N}-1} \frac{\mathcal{N} - |j|}{\mathcal{N}} [G(|jp + t|) + G(|jp - t|) - 2G(|jp|)] = 2G(t) \quad (36)$$

$$+ 2 \sum_{j=1}^{\mathcal{N}-1} \frac{\mathcal{N} - j}{\mathcal{N}} [G(jp + t) + G(jp - t) - 2G(jp)] = 2G(t) + 4 \sum_{j=1}^{\mathcal{N}-1} \frac{\mathcal{N} - j}{\mathcal{N}} \sum_{m=1}^{\infty} \frac{t^{2m}}{(2m)!} G^{(2m)}(jp) \quad (37)$$

$$= 2G(t) + 4 \sum_{j=1}^{\mathcal{N}-1} \frac{\mathcal{N} - j}{\mathcal{N}} \sum_{m=1}^{\infty} \frac{t^{2m}}{(2m)!} F^{(2m-1)}(jp), \quad (38)$$

where we have introduced the derivative of  $G$ :

$$F(x) := \int_0^\infty dq \frac{1 - e^{-xq}}{\cosh^2(q/4)} \quad (39)$$

$$= 8x(H_x - H_{x-\frac{1}{2}}), \quad (40)$$

where  $H_x$  is the harmonic number (see Appendix D for the steps to solve the integral). The Taylor series converges for all  $t, p$ , and  $\mathcal{N}$  and the derivatives  $F^{(n)}(x)$  are easy to calculate and to evaluate. It is useful to note that  $F^{(n)}(x)$  are all positive (negative) for odd (even)  $n$ , finite for  $x \in [0, \infty]$ , and monotonically approaching 0 as  $x \rightarrow \infty$ . We estimate the error by the Lagrange error bound for Taylor series, which

states that the error  $E_n$  by approximating a function  $f$  at a position  $x$  using a Taylor series of order  $n$  around  $x_0$  has an upper bound of

$$E_n \leq \frac{\max_{x' \in [x_0, x]} |f^{(n+1)}(x')|}{(n+1)!} |x - x_0|^{(n+1)}. \quad (41)$$

Inserting this back, we obtain the formula for approximating  $\sigma_d^{(1)}$  up to order  $M$

$$\sigma_d^{(1)}(M) = \frac{\mu_0 M_s^2 \Delta_0}{4t} \times \left( G(t) + 2 \sum_{j=1}^{\mathcal{N}-1} \frac{\mathcal{N} - j}{\mathcal{N}} \sum_{m=1}^M \frac{t^{2m}}{(2m)!} F^{(2m-1)}(jp) \right) \quad (42)$$

with the error

$$\Delta \sigma_d^{(1)}(M) = \frac{\mu_0 M_s^2 \Delta_0}{2t} \times \sum_{j=1}^{\mathcal{N}-1} \frac{\mathcal{N} - j}{\mathcal{N}} \frac{t^{2M+1}}{(2M+1)!} |F^{(2M)}(jp - t)|, \quad (43)$$

where we have used that  $F^{(2m)}$  is monotonic to derive the maximum that enters Eq. (41).

From Eqs. (11) and (42) we can now derive the transverse anisotropy constant. For the general case of variable  $\mathcal{N}$  and arbitrary  $t$  and  $p$ , the anisotropy constant  $K_\perp$  is plotted in Fig. 2. We find that this hyperdimensional dependency can be very well approximated by the simple rational form given in Eq. (4). The error made by this approximation is plotted in Fig. 3 for  $\log_{10}(t\mathcal{N})$  in the range of  $-4$ – $5$  in steps of  $0.05$ ,  $\log_2 \mathcal{N}$  in the range of  $0$ – $7$  in unit steps and  $\tau$  in the range of  $1$ – $8$  in steps of  $0.25$ . The error is always smaller than  $9\%$ . That is, for most multilayer systems investigated today, Eq. (4)

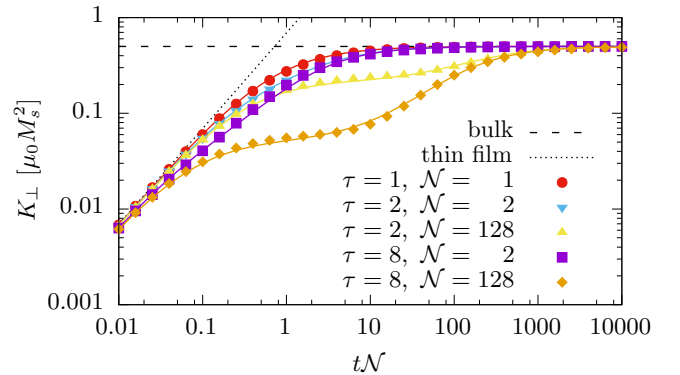


FIG. 2. (Color online) Transverse anisotropy constant  $K_\perp$  as a function of the reduced single layer thickness  $t$ , the reduced layer periodicity  $p$ , and the total number of layers  $\mathcal{N}$  (points). The solid lines show the approximations according to Eq. (4). The dashed line shows the approximation of a very thick (bulk) sample and the dotted line indicates the results of the thin film approximation. Both approximations are significantly inaccurate in the technologically relevant region of multilayers of intermediate thickness.

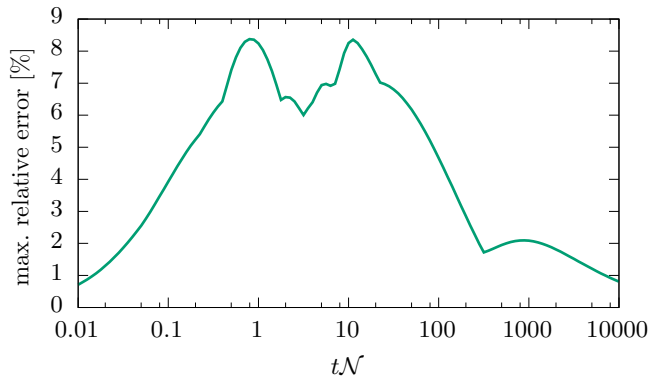


FIG. 3. (Color online) Maximum error made by the approximation of Eq. (4), compared to the accurate result of Eq. (42), as a function of  $tN$  for  $N$  in the range of 1–128 and  $\tau$  in the range of 1–8.

provides a very good description of the transverse anisotropy constant.

## V. APPLICATIONS

We first note that, for a single homogeneous magnetic film, Eq. (42) simplifies to

$$K_{\perp}(N=1) = \frac{\mu_0 M_s^2}{8t} G(t), \quad (44)$$

which converges to  $K_{\perp} = \mu_0 M_s^2/2$  for a bulk material ( $t = \infty$ ) and to  $K_{\perp} = \ln(2)t\mu_0 M_s^2$  for a very thin film ( $t \rightarrow 0$ ), as expected. Also the calculations of Refs. [6] and [7] are well reproduced. However, these measurements and simulations are still well described by the thin film limit for the transverse anisotropy.

The most important application of our calculations is the case of a true multilayer system, i.e., for  $N > 1$ . An example is a Pt(2)/[Co<sub>68</sub>B<sub>32</sub>(0.4)/Pt(0.7)]<sub>30</sub>/Pt(1.3) (thickness in nm) magnetic multilayer with  $M_s = 1.19(3) \times 10^6$  A/m and  $\Delta_0 = 11(2)$  nm, which has been used in the investigation of domain dynamics [1,19]. Entering this into our calculation, we find that the transverse anisotropy constant is given by  $0.07(2)\mu_0 M_s^2$ . This value is a factor of seven smaller than predicted by the simple and widely used formula  $K_{\perp} = \mu_0 M_s^2/2$  and a factor of 1.7 smaller than predicted by the thin film formula  $K_{\perp} = \ln(2)t\mu_0 M_s^2$ . This means that quantitative predictions of the domain wall dynamics, such as the Walker breakdown [10], are inaccurate when relying on existing formulas, showing that one needs to take into account our calculations for a realistic calculation of the resulting domain wall dynamics.

The actual purpose of  $K_{\perp}$  is to describe the stray field energy associated with small tilt angles  $s = \sin^2 \psi$ . However, this small angle assumption is usually ignored when using  $K_{\perp}$  in the one-dimensional model [9,10]. The only higher-order correction that is taken into account is the change of domain wall width with  $s$ :

$$\Delta(s) = \sqrt{A/(K_{u,\text{eff}} + sK_{\perp})}. \quad (45)$$

Within this approximation, the stray field energy is given by

$$\sigma_d(s) = C + 2\Delta(s)K_{\perp}s \quad (46)$$

It is common practice to use this approximation in the one-dimensional model irrespective of the size of  $s$  [10]. In particular, the Walker breakdown is characterized by  $s$  continuously oscillating between 0 and 1. Within the approximation Eq (46), one can calculate the Walker breakdown field for given  $K_{\perp}$ ,  $\alpha$ , and  $M_s$  as [10,20,21]

$$H_W = \frac{\alpha K_{\perp}}{\mu_0 M_s} \quad (47)$$

and the Walker breakdown current density  $J_W$  from given  $K_{\perp}$ ,  $\alpha$ ,  $M_s$ , nonadiabatic parameter  $\beta$ , and spin polarization of the material  $P$  as [9,10,22]

$$J_W = \frac{2eK_{\perp}\Delta(s=0.5)}{\hbar P} \frac{\alpha}{|\beta - \alpha|}, \quad (48)$$

where  $e = 1.6 \times 10^{-11}$  C is the elementary charge, and  $\hbar = 1.05 \times 10^{-34}$  Js is the reduced Planck constant. Note that  $J_W$  might differ slightly from the current density  $J_{\text{max}}$  corresponding to the maximum velocity [9].

With the extension to all angles  $s$ , our model can also be applied to domain walls in systems with Dzyaloshinskii-Moriya interaction (DMI) [23–26]. These systems are particularly exciting since the chiral DMI interaction acts as an additional degree of freedom stabilizing domain walls of a given chirality. This chiral interaction has to be taken into account as an effective magnetic field in the  $x$  direction in the one-dimensional model [24]. Therefore, the accurate knowledge of  $K_{\perp}$  allows the determination of other parameters, such as the Gilbert damping, the spin polarization, or the DMI strength, from measurements of the domain wall velocity versus field or current amplitude.

Finally, the in-plane stray field of a domain wall is used in a novel magnetic imaging technique that detects this stray field via the Zeeman-splitting of the electronic energy levels of a nitrogen vacancy in diamond [27]. Such measurements allow the determination of the domain wall angle  $\psi$  by comparing the measured stray field with the calculated stray field as a function of  $\psi$ . We envision that the mathematical concepts presented here are helpful to obtain more accurate formulas for the theoretical stray field, thus enabling more accurate direct measurements of the spin structure of domain walls in out-of-plane magnetized multilayers.

## VI. CONCLUSIONS

In conclusion, we have derived an accurate analytical expression for the transverse anisotropy constant in perpendicular magnetic multilayer films as used in a 1D model description. The transverse anisotropy constant can be reliably computed using magnetic properties that can be ascertained easily for multilayer films from static measurements. We have shown that the results can significantly deviate from existing and commonly used theories that oversimplify the actual sample configuration and are only valid in the very thin or very thick limit but not in the intermediate regime, which is, however, most widely used for devices. We have provided a more accurate simplification yielding sufficiently precise results for most systems investigated today that are easily accessible without very involved computation. In particular we show that for a commonly used multilayer stack our result

describes the anisotropy well compared to the conventionally used approximations, which are off by up to a factor of seven.

Our results enable precise modeling of domain wall dynamics in systems with perpendicular magnetic anisotropy using the 1D model, which has previously failed due to inaccurate assumptions of the transverse anisotropy. Our model can be applied to determine various material parameters, such as the Gilbert damping, the spin polarization, or the DMI strength, from current- or field-driven domain wall motion experiments.

### ACKNOWLEDGMENTS

This work was funded by the German Ministry for Education and Science (BMBF) through the projects MULTIMAG (13N9911) and MPSCATT (05K10KTB), EU's 7th Framework Programme MAGWIRE (FP7-ICT-2009-5 257707) and WALL (FP7-PEOPLE-2013-ITN), the European Research Council through the Starting Independent Researcher Grant MASPIC (ERC-2007-StG 208162), the Mainz Center for Complex Materials (COMATT and CINEMA), the Graduate School Materials Science in Mainz (GSC/266) and the Deutsche Forschungsgemeinschaft (DFG). B.K. is grateful for financial support by the Carl Zeiss Stiftung.

### APPENDIX A: $y$ INTEGRATION

Here, we will calculate the integral

$$\frac{1}{\mathcal{W}} \int_0^{\mathcal{W}} dy \int_0^{\mathcal{W}} dy' \frac{1}{\sqrt{(y-y')^2 + a}} \quad (\text{A1})$$

for large  $\mathcal{W}$ . The integration with respect to  $y'$  yields

$$\int_0^{\mathcal{W}} dy' \frac{1}{\sqrt{(y-y')^2 + a}} \quad (\text{A2})$$

$$= -\ln(\sqrt{(y-y')^2 + a} + y - y') \Big|_{y'=0}^{\mathcal{W}} \quad (\text{A3})$$

$$= -f(y - \mathcal{W}) + f(y), \quad (\text{A4})$$

$$f(y) = \ln(\sqrt{y^2 + a} + y). \quad (\text{A5})$$

The antiderivative of  $f$  reads

$$F(y) = y \ln(\sqrt{a + y^2} + y) - \sqrt{a + y^2} \quad (\text{A6})$$

and the total integral is therefore given by

$$\frac{1}{\mathcal{W}} \int_0^{\mathcal{W}} dy \int_0^{\mathcal{W}} dy' \frac{1}{\sqrt{(y-y')^2 + a^2}} = (F(\mathcal{W}) + F(-\mathcal{W}) - 2F(0))/\mathcal{W} \quad (\text{A7})$$

$$= \ln(\sqrt{a/\mathcal{W}^2 + 1} + 1) - \ln(\sqrt{a/\mathcal{W}^2 + 1} - 1) \quad (\text{A8})$$

$$- 2\sqrt{a/\mathcal{W}^2 + 1} + 2\sqrt{a/\mathcal{W}^2} \quad (\text{A8})$$

$$= -2 + 2 \ln(2\mathcal{W}) - \ln(a) + \mathcal{O}(\mathcal{W}^{-1}). \quad (\text{A9})$$

### APPENDIX B: FOURIER SPACE IDENTITIES

Here, we show how to reduce a typical double integral over a pair interaction kernel to a single integral in Fourier space

(assuming real-valued functions):

$$\iint dx dx' f(x) h(x') g(x - x') \quad (\text{B1})$$

$$= \int dx f(x) \int dx' g(x - x') h(x') \quad (\text{B2})$$

$$= \int dx f(x) (h * g)(x) \quad (\text{B2})$$

$$= \int dx f(x) \int dk \hat{h}(k) \hat{g}(k) e^{-ikx} \quad (\text{B3})$$

$$= \sqrt{2\pi} \int dk \hat{h}(k) \hat{g}(k) \frac{1}{\sqrt{2\pi}} \int dx f(x) e^{-ikx} \quad (\text{B4})$$

$$= \sqrt{2\pi} \int dk \hat{h}(k) \hat{g}(k) [\hat{f}(k)]^*. \quad (\text{B5})$$

Note that we are using the following definition of the Fourier transform:

$$\hat{f}(k) = \frac{1}{\sqrt{2\pi}} \int dx f(x) e^{ikx} \quad (\text{B6})$$

$$f(x) = \frac{1}{\sqrt{2\pi}} \int dk \hat{f}(k) e^{-ikx}. \quad (\text{B7})$$

### APPENDIX C: $z$ INTEGRATION

In the following we show how to perform the integration of Eq. (29). We first note that

$$\iint e^{-k|z|} dz = k^{-2} (e^{-k|z|} - k|z|) \quad (\text{C1})$$

is a continuous second antiderivative of  $\exp(-k|z|)$ . Furthermore, remember that

$$\int_a^b dz \int_c^d dz' f(z' - z) = G(c - b) + G(d - a) - G(c - a) - G(d - b) \quad (\text{C2})$$

if  $\frac{d^2 G(z)}{dz^2} = f(z)$ . Using these identities, we see that

$$\int_0^T dz \int_0^T dz' \hat{h}(k, z - z' + j\mathcal{P}) \quad (\text{C3})$$

$$= \frac{\sqrt{2\pi}}{|k|} \int_0^T dz \int_0^T dz' e^{-|z-z'+j\mathcal{P}||k|} \quad (\text{C4})$$

$$= \frac{\sqrt{2\pi}}{|k|} \int_0^T dz \int_{-j\mathcal{P}}^{T-j\mathcal{P}} dz' e^{-|z'-z||k|} \quad (\text{C5})$$

$$= \frac{\sqrt{2\pi}}{|k|^3} \sum_{i=-1}^1 (3|i| - 2) (e^{-|j\mathcal{P}+iT||k|} + |j\mathcal{P} + iT||k|). \quad (\text{C6})$$

### APPENDIX D: $q$ INTEGRATION

In this section we provide the exact solution of the Fourier space integral Eq. (34):

$$\int_0^\infty dq \frac{e^{-xq} + xq - 1}{q \cosh^2(q/4)} =: G(x). \quad (\text{D1})$$

To solve this, we note that

$$G(x) = \int_0^x F(x') dx', \quad (D2)$$

where the integral

$$F(x) = \int_0^\infty dq \frac{1 - e^{-xq}}{\cosh^2(q/4)} \quad (D3)$$

$$= 4 - 4 \int_0^\infty dq \underbrace{e^{-xq}}_{f(q)} \underbrace{\frac{e^{q/2}}{(1 + e^{q/2})^2}}_{g'(q)} \quad (D4)$$

$$= 4 \int_0^\infty dq (-x) e^{-xq} \frac{-2}{1 + e^{q/2}} \quad (D5)$$

$$= 8x \int_0^\infty dq e^{-xq} \frac{e^{q/2} - 1}{(e^{q/2} - 1)(e^{q/2} + 1)} \quad (D6)$$

$$= 8x \int_0^\infty dq \frac{e^{-(x-1/2)q} - e^{-xq}}{e^q - 1} \quad (D7)$$

$$= 8x \int dy \frac{y^{x-1/2} - y^x}{1 - y} \quad (D8)$$

$$= 8x (H_x - H_{x-\frac{1}{2}}) \quad (D9)$$

can be solved through integration by parts. Here,  $H$  is the harmonic number. We therefore obtain

$$G(x) = -8 \left\{ \psi^{(-2)}(x+1) - \psi^{(-2)}\left(x + \frac{1}{2}\right) - s \ln(\Gamma(x+1)) + x \ln \left[ \Gamma\left(x + \frac{1}{2}\right) \right] - \psi^{(-2)}(1) + \psi^{(-2)}\left(\frac{1}{2}\right) \right\}, \quad (D10)$$

where  $\Gamma$  is the gamma function and  $\psi$  is the digamma function.

- 
- [1] F. Büttner, C. Moutafis, A. Bisig, P. Wohlhüter, C. M. Günther, J. Mohanty, J. Geilhufe, M. Schneider, C. v. Korff Schmising, S. Schaffert, B. Pfau, M. Hantschmann, M. Riemeier, M. Emmel, S. Finizio, G. Jakob, M. Weigand, J. Rhensius, J. H. Franken, R. Lavrijsen, H. J. M. Swagten, H. Stoll, S. Eisebitt, and M. Kläui, *Phys. Rev. B* **87**, 134422 (2013).
  - [2] S. Emori and G. S. D. Beach, *Appl. Phys. Lett.* **98**, 132508 (2011).
  - [3] W. Zhang, P. K. J. Wong, P. Yan, J. Wu, S. A. Morton, X. R. Wang, X. F. Hu, Y. B. Xu, A. Scholl, A. Young, I. Barsukov, M. Farle, and G. v. d. Laan, *Appl. Phys. Lett.* **103**, 042403 (2013).
  - [4] P. E. Roy and J. Wunderlich, *Appl. Phys. Lett.* **99**, 122504 (2011).
  - [5] S. Jung, W. Kim, T. Lee, K. Lee, and H. Lee, *Appl. Phys. Lett.* **92**, 202508 (2008).
  - [6] S. Fukami, T. Suzuki, N. Ohshima, K. Nagahara, and N. Ishiwata, *J. Appl. Phys.* **103**, 07E718 (2008).
  - [7] S. Fukami, Y. Nakatani, T. Suzuki, K. Nagahara, N. Ohshima, and N. Ishiwata, *Appl. Phys. Lett.* **95**, 232504 (2009).
  - [8] A. P. Malozemoff and J. C. Slonczewski, *Magnetic Domain Walls in Bubble Materials* (Academic Press, New York, 1979).
  - [9] A. Thiaville, Y. Nakatani, J. Miltat, and Y. Suzuki, *Europhys. Lett.* **69**, 990 (2005).
  - [10] O. Boulle, G. Malinowski, and M. Kläui, *Mater. Sci. Eng., R* **72**, 159 (2011).
  - [11] G. Tatara and H. Kohno, *Phys. Rev. Lett.* **92**, 086601 (2004).
  - [12] J. Rhensius, L. Heyne, D. Backes, S. Krzyk, L. J. Heyderman, L. Joly, F. Nolting, and M. Kläui, *Phys. Rev. Lett.* **104**, 067201 (2010).
  - [13] L. Thomas, M. Hayashi, X. Jiang, R. Moriya, C. Rettner, and S. S. P. Parkin, *Nature (London)* **443**, 197 (2006).
  - [14] G. S. D. Beach, C. Nistor, C. Knutson, M. Tsoi, and J. L. Erskine, *Nature Mater.* **4**, 741 (2005).
  - [15] W. Döring, *Z. Naturforsch. A* **3**, 373 (1948).
  - [16] A. Hubert and R. Schäfer, *Magnetic Domains - The Analysis of Magnetic Microstructures* (Springer-Verlag, Berlin, 1998).
  - [17] C. Kooy and U. Enz, *Philips Res. Rep.* **15**, 7 (1960).
  - [18] S. V. Tarasenko, A. Stankiewicz, V. V. Tarasenko, and J. Ferré, *J. Magn. Magn. Mater.* **189**, 19 (1998).
  - [19] F. Büttner, C. Moutafis, M. Schneider, B. Krüger, C. M. Günther, J. Geilhufe, C. v. K. Schmising, J. Mohanty, B. Pfau, S. Schaffert, A. Bisig, M. Foerster, T. Schulz, C. a. F. Vaz, J. H. Franken, H. J. M. Swagten, M. Kläui, and S. Eisebitt, *Nature Phys.* **11**, 225 (2015).
  - [20] A. Mougín, M. Cormier, J. P. Adam, P. J. Metaxas, and J. Ferré, *Europhys. Lett.* **78**, 57007 (2007).
  - [21] P. J. Metaxas, J. P. Jamet, A. Mougín, M. Cormier, J. Ferré, V. Baltz, B. Rodmacq, B. Dieny, and R. L. Stamps, *Phys. Rev. Lett.* **99**, 217208 (2007).
  - [22] G. Tatara, H. Kohno, and J. Shibata, *Phys. Rep.* **468**, 213 (2008).
  - [23] S. Emori, U. Bauer, S. Ahn, E. Martinez, and G. S. D. Beach, *Nature Mater.* **12**, 611 (2013).
  - [24] E. Martinez, S. Emori, N. Perez, L. Torres, and G. S. D. Beach, *J. Appl. Phys.* **115**, 213909 (2014).
  - [25] K. Ryu, L. Thomas, S. Yang, and S. Parkin, *Nature Nanotech.* **8**, 527 (2013).
  - [26] A. Fert, V. Cros, and J. Sampaio, *Nature Nanotech.* **8**, 152 (2013).
  - [27] J.-P. Tetienne, T. Hingant, L. J. Martínez, S. Rohart, A. Thiaville, L. H. Diez, K. Garcia, J.-P. Adam, J.-V. Kim, J.-F. Roch, I. M. Miron, G. Gaudin, L. Vila, B. Ocker, D. Ravelosona, and V. Jacques, *Nature Commun.* **6**, 6733 (2015).